

Coherence properties of a single dipole emitter in diamond

Graham D Marshall^{1,2,5}, Torsten Gaebel², Jonathan C F Matthews³, Jörg Enderlein⁴, Jeremy L O'Brien³ and James R Rabeau^{2,5}

¹ Centre for Ultrahigh bandwidth Devices for Optical Systems, Department of Physics and Astronomy, Macquarie University, NSW 2109, Australia

² MQ Photonics Research Centre, Centre for Quantum Science and Technology, Department of Physics and Astronomy, Macquarie University, NSW 2109, Australia

³ Centre for Quantum Photonics, H H Wills Physics Laboratory and Department of Electrical and Electronic Engineering, University of Bristol, Merchant Venturers Building, Woodland Road, Bristol BS8 1UB, UK

⁴ Georg August University, Department of Physics III, Institute of Physics Friedrich-Hund-Platz 1 37077 Goettingen, Germany
E-mail: graham.d.marshall@gmail.com and james.rabeau@mq.edu.au

New Journal of Physics **13** (2011) 055016 (10pp)

Received 20 October 2010

Published 26 May 2011

Online at <http://www.njp.org/>

doi:10.1088/1367-2630/13/5/055016

Abstract. On-demand, high repetition rate sources of indistinguishable, polarized single photons are the key component for future photonic quantum technologies (O'Brien *et al* 2009 *Nat. Photonics* **3** 687–95). Colour centres in diamond offer a promising solution, and the narrow linewidth of the recently identified nickel-based NE8 centre makes it particularly appealing for realizing the transform-limited sources necessary for quantum interference. Here, we report the characterization of dipole orientation and coherence properties of a single NE8 colour centre in a diamond nanocrystal at room temperature. We observe a single-photon coherence time of 0.21 ps and an emission lifetime of 1.5 ns. Combined with an emission wavelength that is ideally suited for applications in existing quantum optical systems, these results show that NE8 is a far more promising source than the more commonly studied nitrogen-vacancy centre and point the way to the realization of a practical diamond colour centre-based single-photon source.

⁵ Authors to whom any correspondence should be addressed.

Contents

1. Introduction	2
2. Measurement of coherence length	3
3. Measurement of lifetime and dipole properties	5
4. Summary and conclusions	6
Acknowledgments	7
Appendix	7
References	9

1. Introduction

Unwanted photon number states in the spontaneous parametric downconversion (SPDC) process are a detrimental source of noise in current multiphoton experiments [2]. Together with its non-deterministic nature, reliance on SPDC as a source of photons is a major limiting factor in realizing scalable photonic quantum technologies. Leading alternatives include colour centres in solids [3] and quantum dots [4–8]. At cryogenic temperatures, quantum dots fabricated in micro-pillar cavities are capable of emitting transform-limited single photons to demonstrate quantum interference in the two-photon Hong–Ou–Mandel effect [9]. The nitrogen-vacancy (NV) centre in diamond has gained attention in quantum technologies and biological imaging [10–15] for its high quantum yield at room temperature and the polarization-sensitive optical transition of NV that enables manipulation and readout of single-electron and nuclear spins in diamond. In the context of *optical* quantum science however, NV has a number of limitations. An isolated centre typically produces single photons in a broad emission spectrum ~ 100 nm wide with relatively low coupling to the zero-phonon line (ZPL) (the Debye–Waller factor is 0.04 [16])—dispersion makes such a spectrally broad source of light unsuitable for fibre transmission and, as with all free-space single emitters, the collection efficiency is poor. The room temperature NV centre excited-state lifetimes (typically 12–25 ns [17]) are large in comparison to the femtosecond coherence time for the whole wavelength emission band and even the picosecond coherence time for the ZPL alone [18, 19], making it extremely hard to realize a Fourier-transform-limited photon source (i.e. a source of indistinguishable photons) based on NV.

Interest has centred around *single* nickel (Ni) related defects first detected in natural diamond [16] and subsequently synthesized in the laboratory using chemical vapour deposition (CVD) [20]. Further work has generated a rich area of study, with numerous colour centres at a range of spectral positions both with Ni [21, 22] and other defect sites [23, 24] as well as low-temperature investigations of near-IR colour centres [25]. The so-called NE8 centre (figure 1(a)) is best documented in ensembles [26, 27], and *ab initio* density functional theory suggests it is the most stable experimentally measured form of Ni–N complex [28]. NE8 typically has a narrow spectral emission with a full-width half-maximum (FWHM) of less than 3 nm at room temperature and a centre wavelength of approximately 795 nm. These properties make it ideally suited as a replacement for existing SPDC systems that generate photons around 800 nm and where commercially available silicon single-photon avalanche photodiodes have high sensitivity. With its demonstration as a room temperature triggered single-photon source [29], NE8 is a promising candidate to advance optical quantum technologies. However, in order to determine the feasibility of engineering an NE8-based transform-limited source,

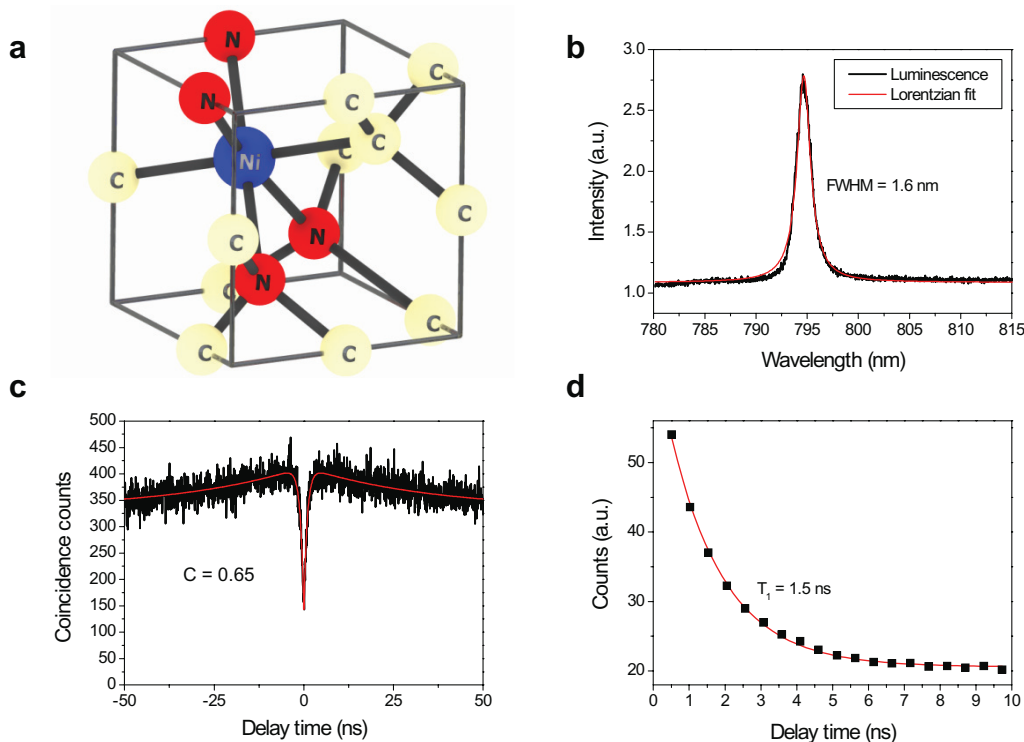


Figure 1. The NE8 colour centre. (a) Structure of NE8. (b) Luminescence spectrum of NE8 (black curve) with a Lorentzian fit (red curve). (c) Second-order correlation function of the luminescence signal, indicating the presence of a single-photon emitter. (d) Luminescence emission as a function of time observed using a pulsed excitation source.

it is essential to be able to measure the orientation of the dipole emitter and characterize the coherence and excited-state lifetime properties of the NE8 centre.

2. Measurement of coherence length

We report the results obtained from a single photostable NE8 centre in CVD-grown diamond nanocrystal and measured using the scanning confocal microscope setup shown in figure 2(a) (full experimental details are included in the [appendix](#)). The measured NE8 luminescence spectrum (figure 1(b)) consists of a single line centred at 794.7 nm, which is consistent with the expected emission wavelength from the NE8 colour centre in diamond [30]. The uncorrected $g^{(2)}$ function (see the [appendix](#)) presented in figure 1(c) shows a contrast greater than 0.5, which indicates the presence of a single emitting centre and phenomena such as background scattering and fluorescence, and detector noise will reduce the contrast value. The saturation intensity data obtained in the CW regime were consistent with those presented in [16], which gives a full and detailed characterization of the NE8 centre, and are not included here.

The lineshape of the luminescence spectrum reveals a 1.6 nm FWHM Lorentzian profile, indicating that photon emission was dominated by the natural lifetime and was not subject to Doppler broadening. The Lorentzian shape and known width of the emission line of the NE8 centre allowed us to make an initial estimate of the coherence properties of emitted photons.

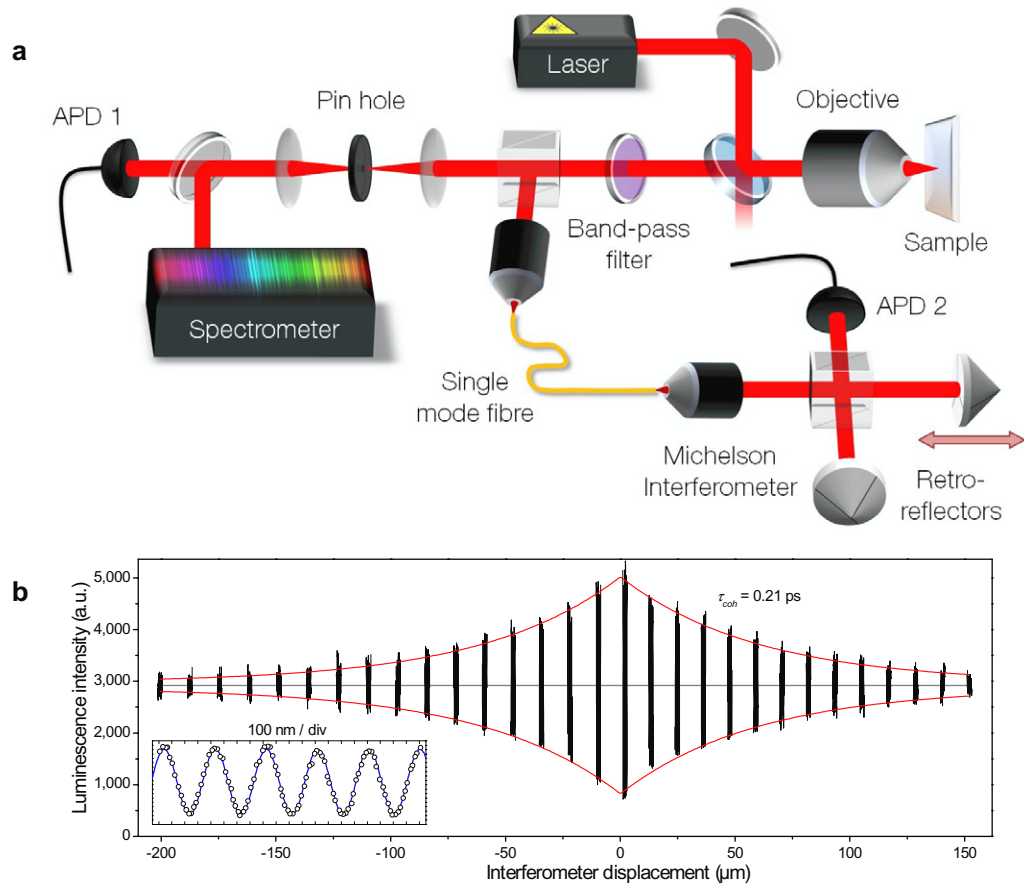


Figure 2. The confocal microscope and measurement of the luminescence coherence length. (a) The scanning confocal microscope collects the luminescence signal, which is delivered, via a 10 m single-mode fibre, to a stabilized Michelson interferometer. Using the interferometer, single photon interference is realised to directly measure the coherence length. (b) The resulting interference pattern envelope and single exponential fit; the inset shows a magnified view of the central interference region fitted with a sine curve.

The coherence length of the single-photon state can be approximated by

$$l_{\text{coh}} = \lambda^2 / 2\pi \Delta\lambda, \quad (1)$$

where $\Delta\lambda$ is the FWHM of the spectrum peak. Using this estimation, the coherence length implied by the luminescence spectrum was $63 \mu\text{m}$; however, factors such as phonon broadening may influence and decrease the coherence length. Until now the optical coherence properties of the NE8 centre have not been measured and speculation has been based on measured emission linewidth.

The coherence length of the room temperature NE8 source was directly measured using a scanning Michelson interferometer (figure 2(a)). By varying the path length in the interferometer about the zeroth-order fringe position, the measurement of the change in interference fringe contrast as a function of path length yielded a direct measurement of the single-photons' coherence length. Single photons were collected by the microscope and passed through a 50 : 50 beam splitter; one arm then proceeded to a confocal pinhole and APD detector, the other to a

single-mode fibre that coupled the light to the interferometer. The advantage of this setup is that it allows the simultaneous measurement of coherence length and second-order correlation function $g^{(2)}$, and in an elegant demonstration of wave–particle duality thereby confirms that the interferometer is measuring the coherence length of single photons. The automated coherence length measurements took approximately 2 h and the sampled interference pattern from a typical scan is shown in figure 2(b). The interference pattern displays a single exponential decay of the ‘carrier’ fringe contrast about the zeroth-order fringe position. Throughout the decay envelope, the fringe carrier frequency was in phase, indicating that the interferometer remained stable.

The shape of the fringe contrast decay curve can be better understood when one considers that the interferometer measures the Fourier transform of the source spectrum. Indeed, the Fourier transform of a Lorentzian curve is a decaying single exponential. The interferometrically measured coherence length of NE8 emission was $63 \mu\text{m}$ (coherence time 0.21 ps). This value was derived from the $1/e$ decay point of the interference pattern envelope maxima and minima fit and is in excellent agreement with the coherence length estimated from the luminescence spectrum.

3. Measurement of lifetime and dipole properties

In addition to having a narrow emission linewidth, one of the other advantages of the NE8 centre over other diamond colour centres is the short lifetime of the excited-state levels. Compared with the known typical lifetimes of 12–25 ns for NV and 2–3 ns for SiV, we measured the NE8 centre as having a lifetime of 1.5 ns (figure 1(d)). Such a short lifetime is ideal for realizing high-brightness single-photon sources.

NE8 has a well-defined single dipole orientation. This is in contrast to centres such as NV where the centre geometry gives rise to orthogonal transition dipoles that are incoherent [31]. It is therefore possible to maximize the NE8 centre luminescence intensity by orientating the excitation beam’s polarization with the state of polarization of the absorption dipole. Furthermore, the emission of the NE8 centre can be expected to have a single linear polarization—a highly desirable property in future applications where the emission from separate centres are interfered. To study the polarization properties of the absorption and emission dipole, a linear polarizer was used in conjunction with a half-waveplate (HWP) in the excitation beam path. Rotating the linear polarization of the excitation beam varies the luminescence intensity sinusoidally (figure 3(b)). Adding a second polarizing filter in the collection arm of the microscope showed that emission from the centre is highly polarized and independent of the excitation polarization (figure 3(c)). The absorption and emission dipoles of the centre were observed to be aligned with each other at $+29 \pm 1^\circ$ to the vertical axis (this being the azimuthal angle, the plane of the sample representing the xy -plane). To measure the polar angle of the dipole, we used a defocused scanned luminescence imaging technique (similar to that used to determine the orientation of emission dipoles in luminescence wide-field imaging [32]). Figure 4 shows the measured and modelled emission profile images at three defocus depths. The model confirmed that the azimuthal orientation of the dipole was approximately 28° and indicated that the polar angle was 40° . This ability to measure the orientation of the NE8 dipole will be critical to future applications wherein optimized sources will require the alignment of the optical dipole with the local field of a cavity mode.

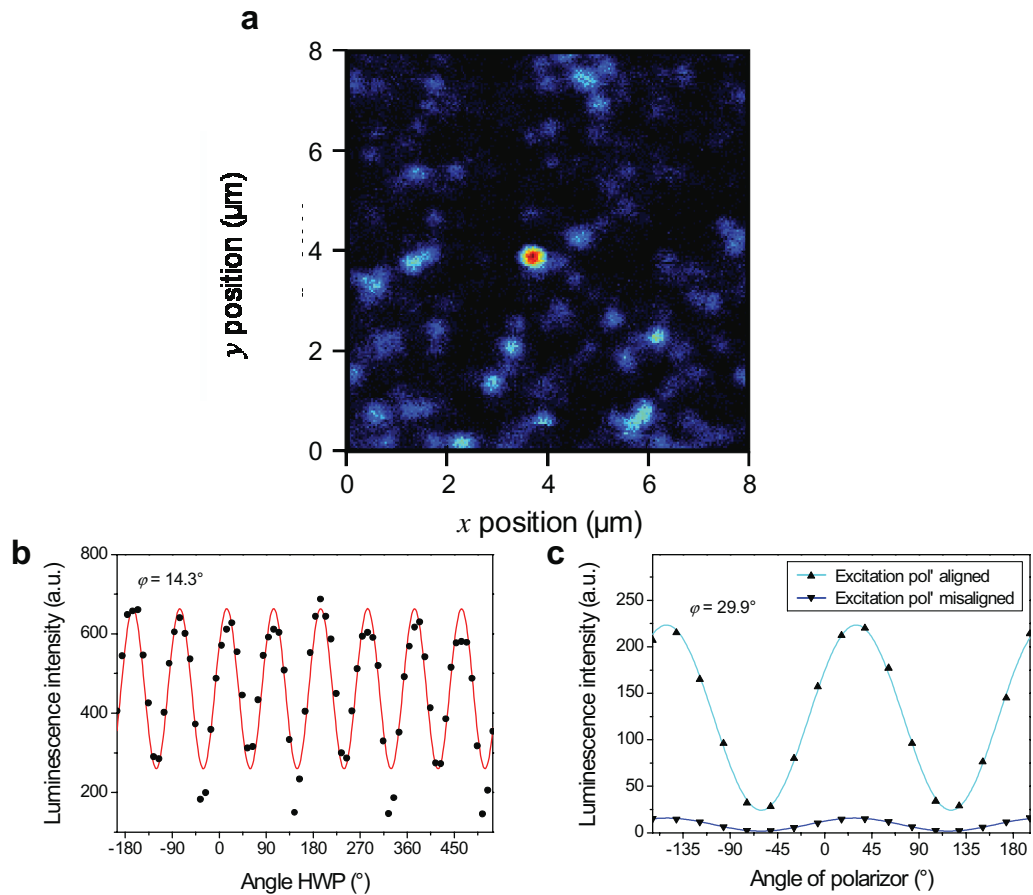


Figure 3. Locating NE8 centres and optical dipole characteristics. (a) A scanning confocal microscope image of the CVD-grown diamond sample and NE8 centre obtained using a band-pass filter. (b) NE8 luminescence signal as a function of excitation beam polarization (black points) with a cosine fit (red curve). (c) Luminescence signal as a function of the angle of a polarizing filter for two different states of excitation polarization.

4. Summary and conclusions

Our results show that the orientation of the NE8 dipole can be precisely measured and that the coherence length shows promise for NE8-based transform-limited sources. These room temperature measurements indicate that the natural excited state lifetime τ_{exc} and coherence time τ_{coh} of NE8 are five orders of magnitude away from the time bandwidth limit given by $2\tau_{\text{exc}}/\tau_{\text{coh}} \approx 1$. Coupling to the evanescent modes of micro-spheres, toroids or photonic crystal cavities, for example, will be a necessary step in developing a transform-limited room temperature source. The ability to measure dipole alignment with the electric field vector is crucial for optimizing the emission efficiency of colour centres coupled to an optical cavity designed to enhance emission rate and increase coherence length. The full potential of single colour centres in diamond for optical applications rests now on the ability to increase the spontaneous emission rate and spectrally narrow the emission line. Combining room temperature photon sources with integrated quantum circuitry [33] and the development of

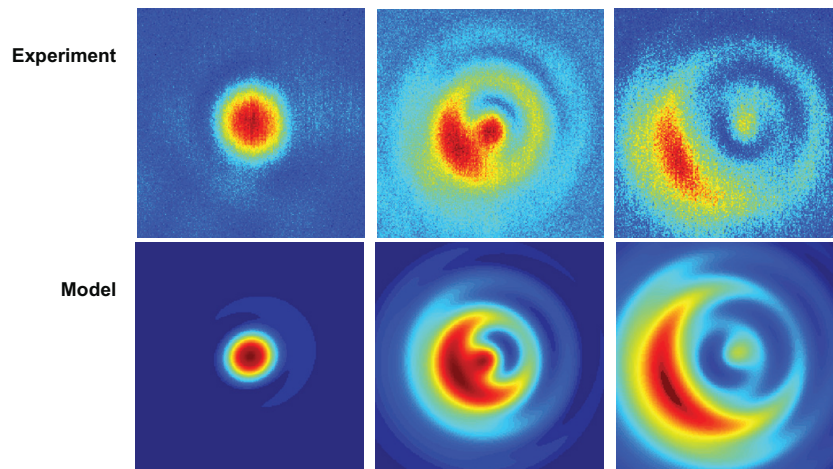


Figure 4. Optical dipole imaging. Images of the dipole emission profile obtained using defocused excitation imaging (top row). The three images (from left to right) were taken at increasing defocus ‘depths’ of 500, 720 and 1320 nm. Theoretical model of the defocused dipole images (bottom row). The model infers a dipole orientation of $\theta = 40^\circ$ and $\varphi = 28^\circ$. The translation field in all images is $2 \mu\text{m} \times 2 \mu\text{m}$.

high-efficiency single-photon detectors [34] are crucial steps towards realizing scalable photonic quantum technologies.

Acknowledgments

We thank J P Hadden, J Harrison, A Politi, J G Rarity and M J Withford for their helpful discussions. Diamond samples were prepared by JRR using the AsTex CVD system at the University of Melbourne. This work was supported by the Australian Research Council (through their Centres of Excellence, Discovery and Future Fellowships programs), the Australian Academy of Science (through their International Science Linkages, Scientific visits to Europe scheme), EPSRC, ERC, the Leverhulme Trust, and the EU under IST-034368 EQUIND. JLO’B acknowledges a Royal Society Wolfson Merit Award.

Appendix

The confocal microscope used in this study (figure 2(a)) consisted of an xyz -scanning Olympus UPlanApo 100×1.3 NA oil immersion lens and a spatial filter containing a $50 \mu\text{m}$ pinhole. A 40 nm band-pass filter centred at 800 nm was used to filter the excitation light from the luminescence signal. A continuous-wave 685 nm laser diode was fibre coupled and its light was delivered to the microscope via a 700 nm short-pass filter that was used to remove any auto-luminescence originating from the coupling fibre. An uncoated quartz flat was used to reflect a portion of the excitation beam into the microscope while allowing the majority of the luminescence signal to remain in the microscope. The excitation power used during experiments was typically $500 \mu\text{W}$ (measured in front of the focusing objective).

Fabrication of the diamond samples using CVD has been reported previously [20]. A 3 nm bandwidth filter centred at 795 nm was used during the confocal scans for easy discrimination of the NE8 colour centres. This filter was removed for all subsequent measurements with the exception of the dipole-imaging scans.

The azimuthal angle of the dipole absorption was determined by inserting a Glan-air polarizing prism in the excitation beam path in front of the turning quartz-flat. An HWP was then inserted in front of the focusing objective. The HWP imparts an angle of rotation to the linearly polarized beam that is twice the waveplate physical orientation; hence the cosine fit in figure 3(b) has a phase angle, 14.3° , that is half the absorption dipole azimuthal orientation. (The contrast of this measurement was limited by the zero-order HWP design wavelength, which was 800 nm and not 685 nm.) By positioning the HWP before the quartz-flat and adjusting the laser diode current to maintain the same excitation power, the angle of the emission dipole was measured at two different linear excitation polarizations. Using a linearly polarizing filter in the detector path, we observed the polarization angle of the luminescence to be independent of the angle of the excitation light's polarization. In figure 3(c), the luminescence signal intensity with polarization angle for two different excitation polarizations is shown. The phase of the two cosine fit curves, 29.9° , is the same (within error) and is the emission dipole azimuthal orientation.

To measure the excited-state lifetime (T_1) of the nickel colour centre, we replaced the CW red excitation laser diode with a 130 ps pulsed 730 nm laser diode, the light from which was delivered via the same optical fibre as used for the red excitation. The luminescence from the colour centre was then recorded using a time-correlated single-photon-counting (TCSPC) system (PicoQuant PicoHarp). After allowing for a short period when scattered light is detected by the TCSPC detector, the decay of the luminescence signal follows a single exponential curve with decay constant measured to be 1.5 ns (figure 1(c)).

A Hanbury Brown and Twiss (HBT) interferometer was used to measure the second-order correlation function $g^{(2)}(\tau) = \langle I(t)I(t+\tau)/I(t)^2 \rangle$, which gives an indication of the number of emitters in a particular nanocrystal. $g^{(2)}(\tau)$ is the probability of detecting two simultaneous photons (where $\tau = 0$) normalized by the probability of detecting two photons at once for a random photon source: an 'antibunching' dip in $g^{(2)}(\tau)$ indicates sub-Poissonian statistics of the emitted photons and reveals the presence of a single quantum-system that cannot simultaneously emit two photons. The contrast in $g^{(2)}(\tau)$ (for this centre it was 0.65 ± 0.03 —see figure 1(c)) scales as $1/N$, where N is the number of emitters [11, 35]. Note that in this experiment $g^{(2)}(\tau)$ was measured via the optical fibre link between the confocal microscope and interferometer APDs, thereby ensuring that the Michelson interferometer measured the coherence length of the single photons emitted by the NE8 centre.

To measure the coherence length of NE8 photons, the single-mode optical fibre was connected to the input of a bulk-optical Michelson interferometer comprising a 50 : 50 beam splitter and two corner-cube retroreflectors (figure 2(a)). To obtain a representative sample of the full NE8 interference pattern (figure 2(b)), we employed a step-and-scan technique. The measurement retroreflector of the interferometer was carried on top of a motorized translation stage that included a short-range high-resolution piezo flexure. Step increments in the interferometer path length were made using the motor before scanning the retroreflector position using the piezo actuator. This technique enabled us to rapidly obtain the form of the envelope function of the interference pattern while fully resolving the interference fringes. A Michelson interferometer performs an autocorrelation of an input light field; hence the

interference fringe pattern is symmetric about the zeroth-order fringe and a displacement of the measurement arm mirror imparts twice the path length shift due to its retroreflective nature.

References

- [1] O'Brien J L, Furusawa A and Vuckovic J 2009 Photonic quantum technologies *Nat. Photonics* **3** 687–95
- [2] Prevedel R, Cronenberg G, Tame M S, Paternostro M, Walther P, Kim M S and Zeilinger A 2009 Experimental realization of dicke states of up to six qubits for multiparty quantum networking *Phys. Rev. Lett.* **103** 020503
- [3] Beveratos A, Kuhn S, Brouri R, Gacoin T, Poizat J P and Grangier P 2002 Room temperature stable single-photon source *Eur. Phys. J. D* **18** 191–6
- [4] Gerard J M and Gayral B 1999 Strong purcell effect for InAs quantum boxes in three-dimensional solid-state microcavities *J. Lightw. Technol.* **17** 2089–95
- [5] Michler P, Kiraz A, Becher C, Schoenfeld W V, Petroff P M, Zhang L D, Hu E and Imamoglu A 2000 A quantum dot single-photon turnstile device *Science* **290** 2282–5
- [6] Santori C, Pelton M, Solomon G, Dale Y and Yamamoto E 2001 Triggered single photons from a quantum dot *Phys. Rev. Lett.* **86** 1502–5
- [7] Yuan Z L, Kardynal B E, Stevenson R M, Shields A J, Lobo C J, Cooper K, Beattie N S, Ritchie D A and Pepper M 2002 Electrically driven single-photon source *Science* **295** 102–5
- [8] Zwiller V, Blom H, Jonsson P, Panev N, Jeppesen S, Tsegaye T, Goobar E, Pistol M E, Samuelson L and Bjork G 2001 Single quantum dots emit single photons at a time: antibunching experiments *Appl. Phys. Lett.* **78** 2476–8
- [9] Santori C, Fattal D, Vuckovic J, Solomon G S and Yamamoto Y 2002 Indistinguishable photons from a single-photon device *Nature* **419** 594–7
- [10] Balasubramanian G *et al* 2008 Nanoscale imaging magnetometry with diamond spins under ambient conditions *Nature* **455** 648–U646
- [11] Kurtsiefer C, Mayer S, Zarda P and Weinfurter H 2000 Stable solid-state source of single photons *Phys. Rev. Lett.* **85** 290–3
- [12] Maze J R *et al* 2008 Nanoscale magnetic sensing with an individual electronic spin in diamond *Nature* **455** 644–7
- [13] Smith B R, Inglis D W, Sandnes B, Rabeau J R, Zvyagin A V, Gruber D, Noble C J, Vogel R, Osawa E and Plakhotnik T 2009 Five-nanometer diamond with luminescent nitrogen-vacancy Defect Centers *Small* **5** 1649–53
- [14] Bradac C, Gaebel T, Naidoo N, Sellars M J, Twamley J, Brown L J, Barnard A S, Plakhotnik T, Zvyagin A V and Rabeau J R 2010 Observation and control of blinking nitrogen-vacancy centres in discrete nanodiamonds *Nat. Nanotechnol.* **5** 345–9
- [15] Hadden J P, Harrison J P, Stanley-Clarke A C, Marseglia L, Ho Y-L D, Patton B R, O'Brien J L and Rarity J G 2010 Strongly enhanced photon collection from diamond defect centres under micro-fabricated integrated solid immersion lenses *Appl. Phys. Lett.* **97** 241901
- [16] Gaebel T, Popa I, Gruber A, Domhan M, Jelezko F and Wrachtrup J 2004 Stable single-photon source in the near infrared *New J. Phys.* **6** 98
- [17] Beveratos A, Brouri R, Gacoin T, Poizat J P and Grangier P 2001 Nonclassical radiation from diamond nanocrystals *Phys. Rev. A* **6406** 061802
- [18] Braig C, Zarda P, Kurtsiefer C and Weinfurter H 2003 Experimental demonstration of complementarity with single photons *Appl. Phys. B* **76** 113–6
- [19] Jelezko F, Volkmer A, Popa I, Rebane K K and Wrachtrup J 2003 Coherence length of photons from a single quantum system *Phys. Rev. A* **67** 041802
- [20] Rabeau J R, Chin Y L, Praver S, Jelezko F, Gaebel T and Wrachtrup J 2005 Fabrication of single nickel-nitrogen defects in diamond by chemical vapor deposition *Appl. Phys. Lett.* **86** 131926

- [21] Aharonovich I, Zhou C Y, Stacey A, Orwa J, Castelletto S, Simpson D, Greentree A D, Treussart F, Roch J F and Prawer S 2009 Enhanced single-photon emission in the near infrared from a diamond color center *Phys. Rev. B: Condens. Matter* **79** 235316
- [22] Aharonovich I, Zhou C Y, Stacey A, Treussart F, Roch J F and Prawer S 2008 Formation of color centers in nanodiamonds by plasma assisted diffusion of impurities from the growth substrate *Appl. Phys. Lett.* **93** 243112
- [23] Aharonovich I, Castelletto S, Simpson D A, Stacey A, McCallum J, Greentree A D and Prawer S 2009 Two-level ultrabright single photon emission from diamond nanocrystals *Nano Lett.* **9** 3191–5
- [24] Castelletto S, Aharonovich I, Gibson B C, Johnson B C and Prawer S 2010 Imaging and quantum–efficiency measurement of chromium emitters in diamond *Phys. Rev. Lett.* **105** 217403
- [25] Siyushev P *et al* 2009 Low-temperature optical characterization of a near-infrared single-photon emitter in nanodiamonds *New J. Phys.* **11** 113029
- [26] Nadolinny V A, Yelissev A P, Baker J M, Newton M E, Twitchen D J, Lawson S C, Yuryeva O P and Feigelson B N 1999 A study of C-13 hyperfine structure in the EPR of nickel-nitrogen-containing centres in diamond and correlation with their optical properties *J. Phys.: Condens. Matter* **11** 7357–76
- [27] Yelissev A, Babich Y, Nadolinny V, Fisher D and Feigelson B 2002 Spectroscopic study of HPHT synthetic diamonds, as grown at 1500 degrees C *Diam. Relat. Mater.* **11** 22–37
- [28] Johnston K and Mainwood A 2003 Properties of nickel nitrogen complexes in diamond: stability and electronic structure *Diam. Relat. Mater.* **12** 516–20
- [29] Wu E, Rabeau J R, Roger G, Treussart F, Zeng H, Grangier P, Prawer S and Roch J F 2007 Room temperature triggered single-photon source in the near infrared *New J. Phys.* **9** 434
- [30] Zaitsev A 2001 *Optical Properties of Diamond* (Berlin: Springer)
- [31] Epstein R J, Mendoza F M, Kato Y K and Awschalom D D 2005 Anisotropic interactions of a single spin and dark-spin spectroscopy in diamond *Nat. Phys.* **1** 94–8
- [32] Patra D, Gregor I and Enderlein J 2004 Image analysis of defocused single-molecule images for three-dimensional molecule orientation studies *J. Phys. Chem. A* **108** 6836–41
- [33] Politi A, Matthews J C F, Thompson M G and O’Brien J L 2009 Integrated quantum photonics *IEEE J. Sel. Top. Quantum Electron.* **15** 1673–84
- [34] Migdall A and Dowling J 2004 Introduction to Journal of Modern Optics Special Issue on single-photon detectors, applications, and measurement methods *J. Mod. Opt.* **51** 1265–6
- [35] Brouri R, Beveratos A, Poizat J P and Grangier P 2000 Photon antibunching in the fluorescence of individual color centers in diamond *Opt. Lett.* **25** 1294–96